RMetS
Royal Meteorological Society

Notes and Correspondence
Discerning deep and shallow Adriatic bora events

Milivoj Kuzmić,[a]* Branko Grisogono,[b] XiaoMing Li[c] and Susanne Lehner[d]

[a]*Satellite Oceanography Laboratory, Division of Marine and Environmental Research, Ruđer Bošković Institute, Zagreb, Croatia*
[b]*Faculty of Science, Andrija Mohorovičić Geophysical Institute, University of Zagreb, Croatia*
[c]*Institute of Remote Sensing and Digital Earth, Chinese Academy of Sciences, Beijing, China*
[d]*Remote Sensing Technology Institute (IMF), Earth Observation Center, German Aerospace Center (DLR), Wessling, Germany*

*Correspondence to: Milivoj Kuzmić. E-mail: kuzmic@rudjer.irb.hr

This note examines two Adriatic bora events recorded in TerraSAR-X (TS-X) images taken in the winters of 2011 (Case 1) and 2012 (Case 2). In Case 1, the TS-X captured an image of a deep anticyclonic bora, whereas in Case 2 a shallow cyclonic bora was sampled. High-resolution TS-X images resolved the finer bora spatial structure to a scale of ≈1 km, which has not previously been reported in bora research. In particular, the structures in Case 2 appear to be driven by surface convective heat fluxes caused by substantial temperature differences between the relatively high sea surface temperature (SST) and the overflowing very cold air. The Weather Research and Forecasting (WRF) model simulations used to aid the analyses suggest that the very low upwind 2m temperature in Case 2 reinforced the orographic wave breaking by enhancing the cross-mountain pressure gradient. The ensuing strong cross-mountain flow was responsible for the appearance of secondary jets in the lee of Mount Velebit, for which the TS-X Case 2 scene provides the first satellite-borne evidence.

Key Words: bora wind; Adriatic Sea; TerraSAR-X; WRF model

Received 28 January 2014; Revised 28 April 2015; Accepted 5 May 2015; Published online in Wiley Online Library

1. Introduction

The bora is a gusty, cold and usually dry downslope wind blowing over the Adriatic Sea from northeasterly directions (the lee side of the Dinaric Alps). Orographic wave steepening, overturning, and eventual breaking play an important role in its development (Smith, 1987). Grubišić (2004) presents an observational and modelling study of a bora event that occurred in this area. Her study indicates that downstream of the high peaks a hydraulic jump occurs in the boundary layer (BL), creating near-surface wakes, whereas downstream of the mountain passes the BL flow maintains a high wind speed, resembling a supercritical flow. Jiang and Doyle (2005) also found that in the lee of the passes, the fast BL flow is supercritical, which enables the flow to maintain its speed in the absence of a hydraulic jump. Enger and Grisogono (1998) show the importance of the surface temperature difference (TD) between the upwind and downwind side of a bora flow.

Alpers *et al.* (2009) investigated bora events over the Adriatic Sea and Black Sea using Synthetic Aperture Radar (SAR) images acquired by the Advanced SAR (ASAR) instrument and found the ASAR instrument capable of resolving bora-induced wind jets and wakes. To describe the structure of bora jets over the northern Adriatic Sea, Signell *et al.* (2010) compared SAR-retrieved wind fields with outputs from two numerical models, noting the models' accurate capturing of the jet morphology. Kuzmić *et al.* (2013) report on the early results of TerraSAR-X (SAR using X-band wavelength; TS-X) observations of the Adriatic bora wind.

The purpose of this note is to examine the differences observed between two Adriatic bora events that took place in the winters of 2011 and 2012, using scenes recorded by the TS-X instrument and the WRF model to aid the analysis.

2. Satellite data

Two TS-X scenes related to bora events were collected over the Eastern Adriatic Sea (Figure 1). Radiometrically corrected intensities (in decibels) are displayed with the lower (brighter) tail of the grayscale denoting the strong, and upper (darker) tail the weak wind (presented later in Figure 3). The scenes were acquired in ScanSAR mode and averaged down to a 500 m spatial resolution during the wind calculation. The sea surface wind was derived using the XMOD2 Geophysical Model Function (GMF) as described in Li and Lehner (2014). The XMOD2 was validated against buoy measurements for wind speed in the range of 0–20 m s^{-1}, exhibiting an absolute bias less than 0.5 m s^{-1} and an RMSE less than 1.5 m s^{-1}. To avoid problems with low backscatter, the wind direction from model simulations was used in XMOD2 instead of a scene feature alignment. To this end, as well as to aid the scenes analysis, we used the WRF model (Skamarock *et al.*, 2008) with the set-up described in Kuzmić *et al.* (2013). An important implementation difference was an increase in the number of model domains to four (horizontal

© 2015 Royal Meteorological Society

Uncorrected Proofs

Color Figure - Online only

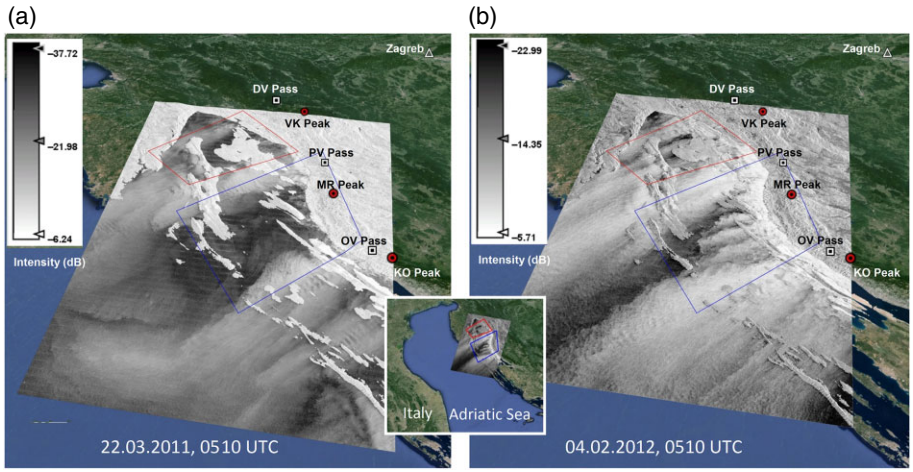

Figure 1. (a) Case 1 and (b) Case 2 TS-X NRCS scenes. The inset provides broader geographic location. The brighter greyscale tail denotes the strong wind, and the darker one the weak wind. Also marked are the major peaks (red circles) and passes (white squares): DV = Delnička vrata (742 m), VK = Velika Kapela (1534 m), PV = Prijevoj Vratnik (698 m), MR = Mali Rajinac (1699 m), OV = Oštarijska vrata (927 m), KO = Konjevača (1381 m), and the location of the Zagreb station. Red and blue quadrangles delineate the zones examined in more detail in Figures 2 and 3.

mesh sizes of 13.5, 4.5, 1.5 and 0.5 km respectively). The Case 1 scene was recorded on 22 March 2011, 0510 UTC (Figure 1(a)). The normalised radar cross-section (NRCS) field with a pixel size of 33 m, re-sampled by a factor of 4 in order to reduce speckle, offers a clear rendering of the jet and wake pattern. The two brightest patterns in the image are the two primary jets emanating from the Prijevoj Vratnik (PV) and Oštarijska vrata (OV) passes respectively. The one from the Delnička vrata (DV) is present but barely noticeable. A well-defined broad wake zone is observed downwind of the Mali Rajinac (MR) peak. Further south, a very narrow wake zone, in the lee of the Konjevača (KO) peak, delineates yet another jet. Case 2 (4 February 2012, 0500 UTC) is intriguingly different (Figure 1(b)). The primary jets (DV, PV and OV) are all much more energetic and broader than in Case 1, with the PV and OV jets exhibiting uniform and linear features apparently reflecting finer incisions in the Dinaric mountain chain. Of particular interest are the changes in the wake zones, now narrower and populated with additional jets. Furthermore, there is practically no quiet zone in the coastal strip which is several km wide. In the rest of this note, we further examine the differences between the two cases, focusing on the zones marked in Figure 1 as red and blue quadrangles.

3. Discussion

According to the Deutscher Wetterdienst (DWD) surface analysis (not shown, archived at http://www1.wetter3.de; accessed 20 May 2015), Case 1 was an anticyclonic (AC) bora flow developed under high pressure systems over Russia and Western Europe related to Siberian and Azores anticyclones, respectively. A deep elevated trough developed over the central Mediterranean promoting cold air advection from Central Europe towards the northeast Adriatic. Case 2 was predominantly a shallow cyclonic bora, although with certain elements of the frontal and AC bora types. It was associated with a persistent, higher-level trough stretching from southeast Scandinavia to the western Mediterranean. The contrast between the Case 1 and Case 2 bora was also reflected in the differences between the upwind Froude numbers (1.15 and 0.68 respectively, based on 1200 UTC soundings in Zagreb – Figure 1). Typical Froude numbers for strong or severe boras are 1/4 $<Fr<$ 1 (e.g. Grisogono and Belušić, 2009). In both cases, interwoven patterns of low-level jets (LLJs) and wakes (Figure 1) pertaining to the respective mountain gaps and peaks populate the marine atmospheric boundary layer (MABL). Grubišić (2004) showed that the corresponding potential vorticity banners separate individual bora jets and wakes at a typical scale of L_H ∼10–25 km. The captured scenes exhibit a richness of detail, showing ever-finer bora spatial structures down to L_H ∼1 km entering the sub-mesoscale, between the largest turbulence eddy scale (∼O(100 m)) and the smallest meso-gamma scale (∼2 km), since the sub-mesoscale typically relates to phenomena on scales less than 2 km. Bora spatial variability at this scale has not been previously observed.

Case 1 (Figure 2(a,b)) exhibits short wave-like patterns in the lee of islands (Krk, Cres, Lošinj, and Pag), with a wavelength of ∼1–2 km. The patterns are 5–10 km wide and 10–15 km long. A more detailed study is likely to interpret these patterns either as footprints of the shortest bora pulses travelling offshore with a duration of ∼2–3 min, or as imprints of short trapped lee waves in the MABL (e.g. Grisogono and Belušić, 2009). The primary LLJs, several tens of km long, border the wake zones of which the most prominent is in the lee of Velebit (MR peak). This wake is initially 30 km wide, gradually spreading offshore, reaching the lee of the island of Rab and then embracing the southern part of Cres and the whole of the Lošinj islands (Figure 2(b)). The TS-X derived wind fields (Figure 3(a,b)) show that in this case both the Kapela and Velebit wakes are indeed rather quiet. Cases like this one have been reported and studied before, albeit at a coarser spatial scale, based on aircraft and land-based measurements and/or model data (Grubišić, 2004; Gohm and Mayr, 2005; Jiang and Doyle, 2005). The case appears akin to the deep AC bora event analysed in Gohm and Mayr (2005) in which high-resolution model simulations, aided by *in situ* observations and measurements, helped identify the BL separation and surface friction processes as being responsible for the wake formation downstream of mountain heights. In Case 2 (Figure 2(c,d)), the whole MABL is very convective. The primary jets are broad, in agreement with the results of Grubišić (2004), and ∼100 km long. These vigorous LLJs stretch nearly perpendicular to the shoreline, with a progressively finer structure further offshore, i.e. a quasi-cellular pattern that cascades in scale from L_H ∼ 10 km down to ∼1 km. The fine-scale cellular structure appears to be driven by the surface convective heat fluxes caused in the MABL by the substantial TD between the relatively high SST and the overflowing very cold air. The DV jet, about 12 km wide, forcefully reaches Mount Ćićarija. Two additional jets in the lee of Kapela now populate the previously quiet zone between the DV and VP jets, passing over the islands of Krk and Cres. These jets relate to secondary mountain passes and the sharp flanks of the islands. Their speed is typically around 15 m s^{-1} (Figure 3(c)), but exceeds 20 m s^{-1} after the jets cross the island of Cres. In contrast to Case 1, the Velebit wake is now rather narrow and turbulent, and stretches out over the sea for more than 100 km with only moderate widening to ∼25–30 km. Four secondary jets, ∼20–40 km long and separated from each other by 5–10 km (Figure 2(d)), occur between the PV and OV primary jets, and agitate and distort the forehead of

Uncorrected Proofs

© 2015 Royal Meteorological Society

AQ8

Color Figure - Online only

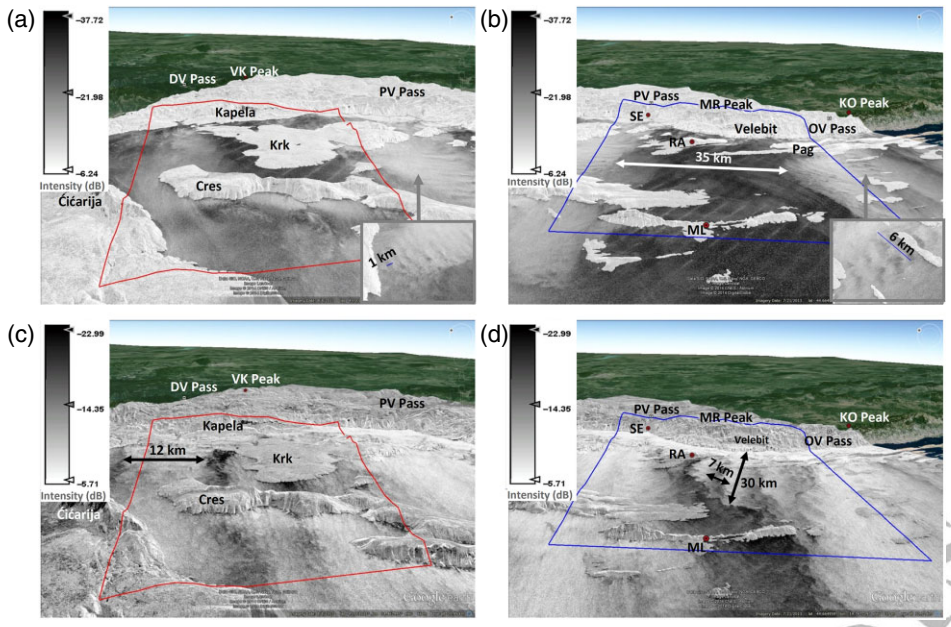

Figure 2. Expension of the TS-X NRCS field in (a) the Case 1 red, (b) Case 1 blue, (c) Case 2 red and (d) Case 2 blue areas (shown in Figure 1). Insets in (a) and (b) provide further details. As in Figure 1, the brighter greyscale tail denotes the strong, and the darker one the weak wind. In both cases the time of the overpass is 0510 UTC. Arrows indicate the size of certain characteristic spatial features. SE, RA, and ML mark the stations where the wind data plotted in Figure 4 were collected.

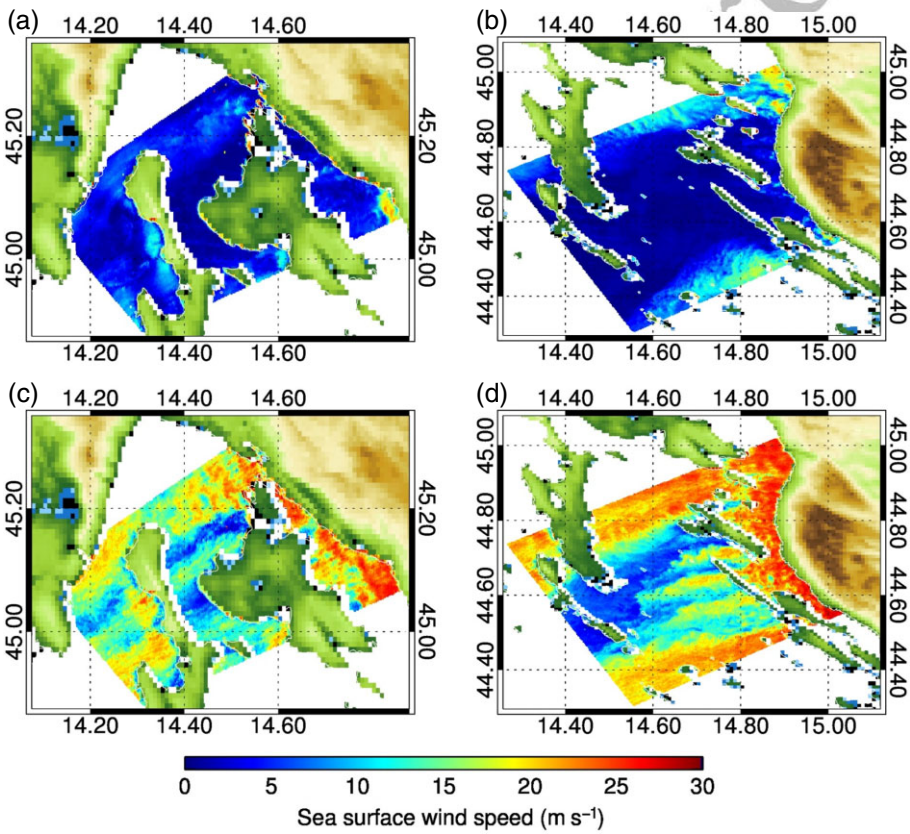

Figure 3. TS-X derived sea surface wind speed in (a) the Case 1 red, (b) Case 1 blue, (c) Case 2 red, and (d) Case 2 blue areas shown in Figures 1 and 2.

the wake, while extending offshore several tens of kilometres. The TS-X derived wind field (Figure 3(d)) indicates that the core of these jet speeds is in excess of 20 m s^{-1}. This case is reminiscent of a strong bora event investigated by Gohm *et al.* (2008). Their April 2002 bora windstorm was also of a shallow, cyclonic type for which numerical simulations suggested that with a strong cross-mountain flow smaller gaps in Mount Velebit could sustain jet flows.

Notwithstanding the wind sheltering at the three measurement stations (Belušić *et al.*, 2013), maxima of 10 min wind speeds, recorded with cup anemometers and 1 s sampling at one coastal (Senj, SE) and two island stations (Rab, RA and Mali Lošinj, ML) reinforce the TS-X results (Figure 4; Figure 2 shows station locations). The plotted 10 min maxima are about twice the 10 min mean values (not shown). The bora is well known for its quasi-periodic gustiness. Belušić *et al.* (2007) point to the Kelvin–Helmholtz instability as the primary mechanism for the pulsations. In Case 1 (Figure 4(a)), the time series show that around the TS-X overpass the bora was weakening, with a clear difference between the stations: SE below the PV jet, and RA and ML in the wake zone. The SE average is still nearly 20 m s^{-1}, whereas RA and ML exhibit values in the 2–4 m s^{-1} range. In

© 2015 Royal Meteorological Society

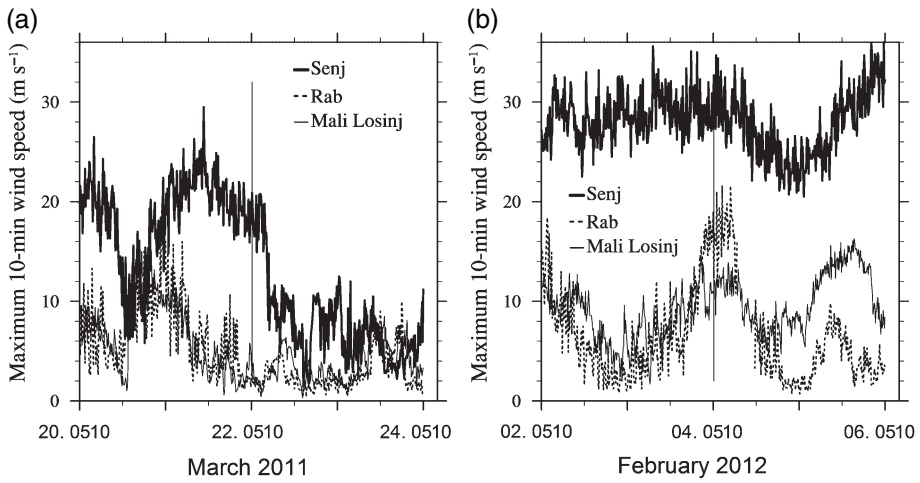

Figure 4. Maximum 10-min wind over a 4-day period centred on TS-X overpass times (0510 UTC) recorded at the Senj, Rab and Mali Lošinj stations (locations marked in Figure 2) for (a) Case 1 and (b) Case 2. Vertical lines mark the TS-X overpass times.

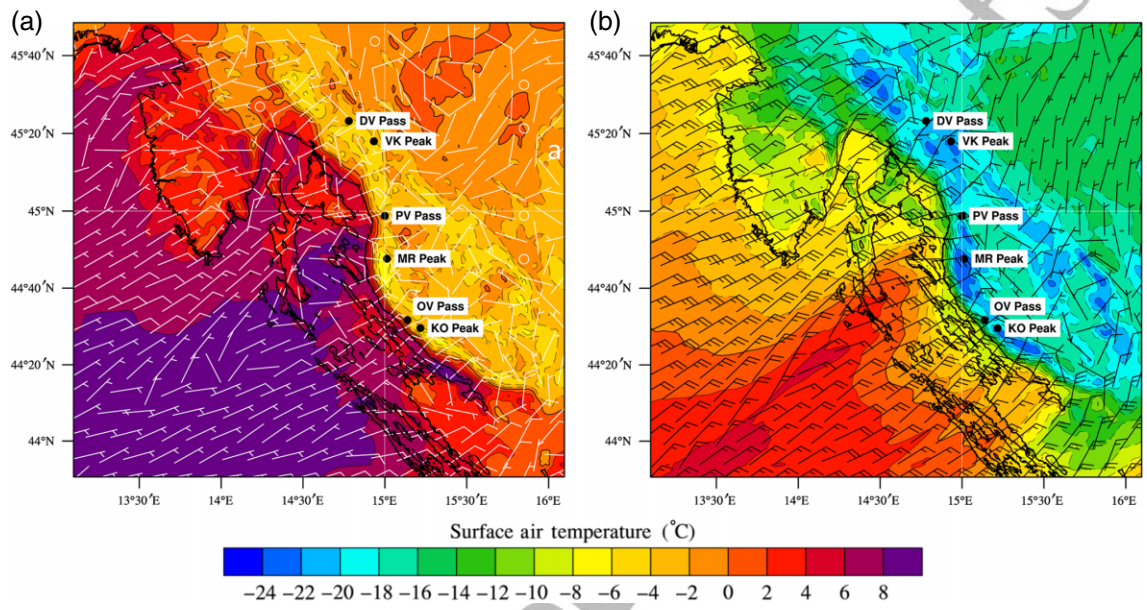

Figure 5. WRF modelled 2 m temperature (colour shading) and 10 m wind fields (arrows) on (a) 22 March 2011, 0500 UTC, and (b) 4 February 2012, 0500 UTC. Also marked are the major peaks and passes: DV = Delnička vrata (742 m), VK = Velika Kapela (1534 m), PV = Prijevoj Vratnik (698 m), MR = Mali Rajinac (1699 m), OV = Oštarijska vrata (927 m), KO = Konjevača (1381 m).

Color Figure - Online only

Case 2, however, the SE 10 min maximum bora, in the 4-day period centred at the TS-X overpass, is nearly 30 m s^{-1}. At the same time, both island stations register lower speeds, although above 10 m s^{-1}. In stark contrast to Case 1, the RA station wind speed is now well above that at ML, apparently reflecting the speed of the westernmost secondary jet, the shortest and slowest of the four. In both cases the wind direction at the SE station during the plotted period was that of the bora (northeasterly), specifically 56° and 68° at the time of the overpass for Case 1 and Case 2 respectively.

In strong to severe bora, a large mountain pressure drag can be related to the blocking of the stably stratified low-level flow upstream of the mountain, often working in concert with a significant wave drag (Smith, 1978). Large surface temperature variations over complex terrain can be a precursor. The idealised study of Enger and Grisogono (1998) show that enhanced land-sea TDs yield more severe bora flows, are associated with more vigorous mountain wave breaking, and give rise to bora front propagation further offshore. To address this aspect further, we take a closer look at the TD between the two cases relying on WRF simulations. Near the surface, the jet-and-wake alternation pattern seen in the NRCS, as well as in the SAR-derived wind fields, is clearly visible in the modelled 10 m wind and the 2m temperature (T_{2m}) field (Figure 5). Notwithstanding reports of WRF underestimating T_{2m} (e.g. Kleczek *et al.*, 2014), one can trace in Case 1 the T_{2m} field (Figure 5(a)) extruding tongues of somewhat cooler air below the PV and OV jets, and a warmer (by approximately 2°C) broad area between them. In Case 2 (Figure 5(b)), the modelled T_{2m} temperature upwind of the Dinaric chain sporadically dropped below −24°C, in a stark contrast to Case 1 where the upwind T_{2m} averaged ≈ −6°C. Furthermore, the offshore T_{2m} was much lower in Case 2, e.g. down to −16°C over the island of Cres, compared to +4 to 6 °C in Case 1. The jet-and-wake pattern in the lee is also noted here, intensified and 'pushed' offshore by a near-coast belt of colder air. WRF vertical temperature transects (not shown) coinciding with Case 1 present a clear but not dramatic division between the marine and continental air, whereas the temperature transect along the same lines in Case 2 exhibits lower temperatures, down to −20°C over the land. It is noteworthy that the 8-day averaged land surface temperature anomaly (LSTA) map over Central and Southeast Europe (http://neo.sci.gsfc.nasa.gov; accessed 20 May 2015) suggests a lack of any serious regional LSTA for Case 1, but shows a pronounced negative LSTA (down to −12°C) in Case 2. The significant surface TDs in Case 2 add to the orographic wave breaking, enhancing the cross-mountain pressure gradient and severe gap-like flows through the coastal mountain passes (e.g. Smith, 1978).

Uncorrected Proofs

© 2015 Royal Meteorological Society

4. Conclusions

In this note, we present a preliminary examination of two Adriatic bora events recorded in two winter TS-X images. The TS-X snapshot taken on 22 March 2011 (Case 1) captured an image of a typical deep anticyclonic bora, whereas the scene recorded on 4 February 2012 (Case 2) sampled a shallow cyclonic bora. In both cases, high-resolution TS-X images resolved the bora structure at a sub-mesoscale that has not been previously reported. In particular, in Case 2 a fine-scale cellular structure appears to be driven by the surface convective heat fluxes caused in the MABL by a substantial TD between the very cold overflowing air and the much warmer sea surface below. The WRF model simulations suggest that the very low upwind T_{2m} in Case 2 reinforced the orographic wave breaking by enhancing the cross-mountain pressure gradient. The strong cross-mountain flow was responsible for the appearance of secondary jets in the lee of Mount Velebit, for which the TS-X Case 2 scene provides the first satellite-borne evidence. Work in progress is focused on further numerical (WRF) modelling of bora events and a better integration of the model and satellite data.

5. Acknowledgements

This work was supported in part by the Croatian Science Foundation as part of the IP-11-2013-5928 and CATURBO No. 09/151 projects. The TerraSAR-X data were collected within the framework of the OCE0478 project. The wind data were kindly provided by the Croatian Meteorological and Hydrological Service. Three anonymous reviewers offered valuable comments which helped to improve the manuscript.

References

Alpers W, Ivanov A, Horstmann J. 2009. Observations of bora events over the Adriatic Sea and Black Sea by spaceborne synthetic aperture radar. *Mon. Weather Rev.* **137**: 1154–1165.

Belušić D, Žagar M, Grisogono B. 2007. Numerical simulation of pulsations in the bora wind. *Q. J. R. Meteorol. Soc.* **133**: 1371–1388.

Belušić D, Hrastinski M, Večenaj Ž, Grisogono B. 2013. Wind regimes associated with a mountain gap at the northeastern Adriatic coast. *J. Appl. Meteorol. Climatol.* **52**: 2089–2105.

Enger L, Grisogono B. 1998. The response of bora-type flow to sea surface temperature. *Q. J. R. Meteorol. Soc.* **124**: 1227–1244.

Gohm A, Mayr G. 2005. Numerical and observational case-study of a deep Adriatic bora. *Q. J. R. Meteorol. Soc.* **131**: 1363–1392.

Gohm A, Mayr GJ, Fix A, Giez A. 2008. On the onset of bora and the formation of rotors and jumps near a mountain gap. *Q. J. R. Meteorol. Soc.* **134**: 21–46.

Grisogono B, Belušić D. 2009. A review of recent advances in understanding the meso- and micro-scale properties of the severe Bora wind. *Tellus* **61A**: 1–16.

Grubišić V. 2004. Bora-driven potential vorticity banners over the Adriatic. *Q. J. R. Meteorol. Soc.* **130**: 2571–2603.

Jiang Q, Doyle JD. 2005. Wave breaking induced surface wakes and jets observed during a bora event. *Geophys. Res. Lett.* **32**: L17807, doi: 10.1029/2005GL022398.

Kleczek MA, Steeneveld G-J, Holtslag AAM. 2014. Evaluation of the Weather Research and Forecasting mesoscale model for GABLS3: Impact of boundary-layer schemes, boundary conditions and spin-up. *Boundary-Layer Meteorol.* **152**: 213–243.

Kuzmić M, Li X-M, Grisogono B, Tomažić I, Lehner S. 2013. TerraSAR-X observations of the northeastern Adriatic bora: Early results. *Acta Adriat.* **54**: 13–26.

Li X-M, Lehner S. 2014. Algorithm for sea surface wind retrieval from TerraSAR-X and TanDEM-X data. *IEEE Trans. Geosci. Remote Sens.* **52**: 2928–2939.

Signell RP, Chiggiato J, Horstmann J, Doyle JD, Pullen J, Askari F. 2010. High-resolution mapping of Bora winds in the northern Adriatic Sea using synthetic aperture radar. *J. Geophys. Res.* **115**: C04020, doi: 10.1029/2009JC005524.

Skamarock WC, Klemp JB, Dudhia J, Gill DO, Barker DM, Duda MG, Huang XY, Weng W, Powers JG. 2008. 'A description of the Advanced Research WRF Version 3', NCAR/TN-475+STR. NCAR: Boulder, CO.

Smith RB. 1978. A measurement of mountain drag. *J. Atmos. Sci.* **35**: 1644–1654.

Smith RB. 1987. Aerial observations of the Yugoslavian Bora. *J. Atmos. Sci.* **44**: 269–297.

Uncorrected Proofs

© 2015 Royal Meteorological Society